

Generation of arbitrary cylindrical vector beams on the higher order Poincaré sphere

Shizhen Chen, Xinxing Zhou, Yachao Liu, Xiaohui Ling, Hailu Luo,* and Shuangchun Wen

¹Key Laboratory for Micro-/Nano-Optoelectronic Devices of Ministry of Education, College of Physics and Microelectronics Science, Hunan University, Changsha 410082, China

*Corresponding author: hailuluo@hnu.edu.cn

Compiled November 6, 2018

We propose and experimentally demonstrate a novel interferometric approach to generate arbitrary cylindrical vector beams on the higher order Poincaré sphere. Our scheme is implemented by collinear superposition of two orthogonal circular polarizations with opposite topological charges. By modifying the amplitude and phase factors of the two beams, respectively, any desired vector beams on the higher order Poincaré sphere with high tunability can be acquired. Our research provides a convenient way to evolve the polarization states in any path on the high order Poincaré sphere.

© 2018 Optical Society of America

OCIS codes: (260.2110) Electromagnetic optics; (260.5430) Polarization.

Light beam with spatially inhomogeneous state of polarization, also referred to as vector beam, has been investigated for many years due to its unique properties [1]. Comparing with the conventional homogeneous polarization represented by fundamental Poincaré sphere, the cylindrical vector beams can be represented by higher order Poincaré sphere (HOPS) [2–4]. Particular interests and investigations focused on the vector beams with radial and azimuthal polarizations, which can be represented as two points on the equator of the first-order Poincaré sphere. Such beams can be generated by twisted nematic liquid crystal [5–7], inserting phase elements in the laser resonator [8], computer-generated sub-wavelength dielectric gratings [9, 10], a conical Brewster prism [11], spatially variable retardation plates [12], and a binary phase mask [13]. The vector beams with special polarization symmetry can give rise to uniquely high-numerical-aperture focusing properties that may find important applications in nanoscale optical imaging and manipulation [14–19].

In this Letter, a novel interferometric method is proposed and experimentally demonstrated to generate arbitrary cylindrical vector beams on the HOPS. Homogeneous polarization on the fundamental Poincaré sphere can be seen as the superposition of two orthogonal circular polarizations corresponding to the two poles of the Poincaré sphere. Similarly, vector beams on the HOPS can be regarded as the linear superposition of two orthogonal circular polarizations with opposite topological charges. For homogenous polarization, two quarter-wave plates (QWPs) and one half-wave plate (HWP) with adjustable optical axis angles can transform it to any point on the fundamental Poincaré sphere [2]. For the HOPS, we use a modified Mach-Zender interferometer with which the amplitude and phase factors in each arm can be modified, respectively.

In the parameter space of the HOPS, the state of polarization ψ_ℓ can be represented by [3]

$$\psi_\ell(v, \phi) = \cos\left(\frac{v}{2}\right)e^{-i\phi/2}L_\ell + \sin\left(\frac{v}{2}\right)e^{i\phi/2}R_\ell. \quad (1)$$

Here, ϕ is the azimuthal angle and v the polar angle in the

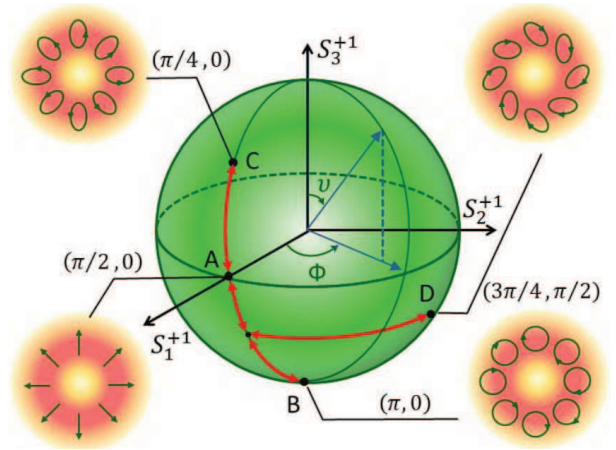


Fig. 1. Schematic illustrating of the first-order Poincaré sphere ($\ell = +1$). The points A, B, C, and D represent four types of vector beams, respectively. The transformations corresponding to the paths AB, AC, and AD are illustrated by the red curve with arrows. The insets show the intensity distribution and the polarization vector (green arrows).

spherical coordinate, respectively. L_ℓ and R_ℓ are orthogonal circular polarization vortices with $L_\ell = (\hat{x} + i\hat{y})e^{-i\ell\varphi}/\sqrt{2}$ and $R_\ell = (\hat{x} - i\hat{y})e^{i\ell\varphi}/\sqrt{2}$, possessing spin angular momentum $\sigma\hbar$ ($\sigma = \pm 1$) per photon where \hbar is the Planck constant. The factor $e^{i\ell\varphi}$ is the vortex phase associated with the orbital angular momentum $\ell\hbar$ per photons where ℓ is an integer number ($\ell = \pm 1, \pm 2, \pm 3, \dots$) [20].

For arbitrary points on the HOPS, the state of polarization $\psi_\ell(v, \phi)$ can be described as the linear combination of two orthogonal circular polarizations with opposite topological charges. Equation (1) indicates that $\cos(v/2)$ and $\sin(v/2)$ are amplitude factors, while $\exp(-i\phi/2)$ and $\exp(i\phi/2)$ are phase factors, respectively. By separately modifying the amplitude and phase factors of the two orthogonal components, any desired vector beam on the HOPS can be achieved. Generally, the equatorial points on the HOPS represent linear polarized

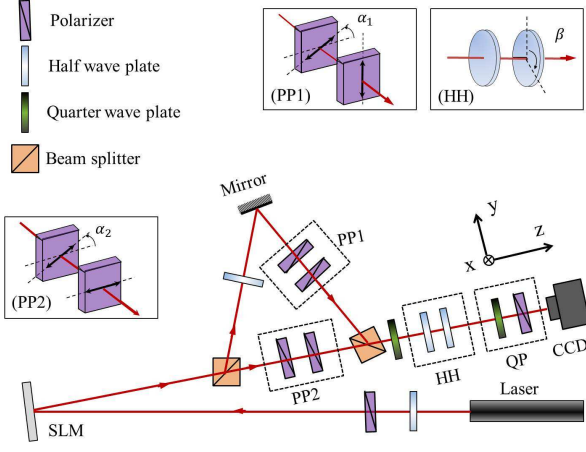


Fig. 2. Experimental setup: Gaussian beam generated by a He-Ne laser (632.8nm, Thorlabs HNL210L-EC) passes through a HWP and a Glan laser polarizer (GLP) to produce a horizontally polarized beam. Then the fundamental Gaussian beam is transformed into a vortex-bearing LG_0^1 mode by a spatial light modulator (SLM) (Holoeye Pluto-Vis). The modified Mach-Zender interferometer comprising of two cascaded beam splitters (BSs) and an odd number of reflections can convert the LG_0^1 mode into LG_0^{-1} mode. In addition, we add PP1 and PP2 (two cascaded GLPs of which the second one is fixed) in each arm of the interferometer to justify the intensity factors. HH (a pair of HWPs within which only the second one can be rotated) is added to modify the phase factors. QP consisting of QWP and GLP, is used to measure Stokes parameters. The intensity distribution of the field is detected by a CCD camera (Coherent LaserCam HR).

vector beams, the two poles denote orthogonal circular polarizations with opposite topological charges, and other points are elliptically polarization, as shown in Fig. 1.

Our experimental setup is plotted in Fig. 2. We use a modified Mach-Zender interferometer, similar to that in Ref. [21], to generate the vector beams. In addition, we employ two cascaded GLPs in each arm to modify the amplitude factors and two cascaded HWPs to modify the phase factors, respectively (see Fig. 2). Modulating the magnitude factor, we can transform the polarization along the longitudes on the HOPS. For northern hemisphere, the relation of ν , α_1 , and α_2 can be written as

$$\alpha_1 = 90^\circ, \quad \cos^2 \alpha_2 = \tan \frac{\nu}{2}, \quad (2)$$

and on southern hemisphere, it becomes

$$\sin^2 \alpha_1 = \cot \frac{\nu}{2}, \quad \alpha_2 = 0^\circ, \quad (3)$$

where α_1 and α_2 are rotation angles with respect to the x axis as illustrated in the insets of Fig. 2. By rotating the second HWP of the HH, we can adjust the phase factors of the vector beams, thereby transforming the polarization along the latitudes on the HOPS. The relation between ϕ and β is given by

$$\beta = \phi/4, \quad (4)$$

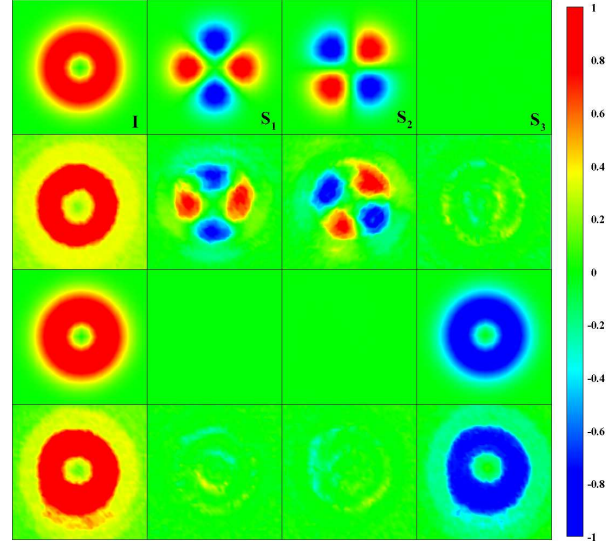


Fig. 3. The Stokes parameters of the generated vector beams corresponding to A and B on the first-order Poincaré sphere (Fig. 1). The first column shows the intensity distribution (S_0) and the next three columns are the Stokes parameters S_1 , S_2 , and S_3 , respectively. First and third rows: the theoretical results for A and B , respectively. Second and fourth rows: the experimental results A and B , respectively.

where β is the rotation angle of the second HWP. With appropriate rotation angles α_1 , α_2 , and β , we can realize arbitrary cylindrical vector beams represented by the corresponding points (ν, ϕ) on the HOPS. This is the main point of the theory.

To examine the polarization of the generated vector beams, we will measure the Stokes parameters by a QP and a CCD camera (see Fig. 2), S_1 , S_2 , and S_3 , which are given by

$$S_1 = \frac{I_{0^\circ}^{0^\circ} - I_{90^\circ}^{90^\circ}}{I_{0^\circ}^{0^\circ} + I_{90^\circ}^{90^\circ}}, S_2 = \frac{I_{45^\circ}^{45^\circ} - I_{135^\circ}^{135^\circ}}{I_{45^\circ}^{45^\circ} + I_{135^\circ}^{135^\circ}}, S_3 = \frac{I_{135^\circ}^{135^\circ} - I_{0^\circ}^{45^\circ}}{I_{135^\circ}^{135^\circ} + I_{0^\circ}^{45^\circ}}, \quad (5)$$

where I_j^i stands for the intensity of the light recorded by the CCD, and i and j are the optical axis directions of the QWP and GLP with respect to the x axis, respectively [22]. Note that the intensity profiles of S_3 depends on the polar angle ν . The linear polarized vector beams represented by the equatorial points of the HOPS have $S_3 = 0$ at each transverse point. And $S_3 = \pm 1$ correspond to circular polarizations. But for the S_1 and S_2 , the intensity patterns are both dependent on the angles ν and ϕ .

We first generate the vector beams on the equator and the south pole (A and B) on the first-order Poincaré sphere as shown in Fig. 1. For the vector beam on the point A ($\nu = \pi/2$ and $\phi = 0$), from Eqs. (2)-(4), we get $\alpha_1 = 90^\circ$, $\alpha_2 = 0^\circ$, and $\beta = 0$. In order to achieve the vector beam on the points B , we must ensure that $\alpha_1 = 0^\circ$, $\alpha_2 = 0^\circ$, and β be an arbitrary value. The Stokes parameters of the generated beams are measured to verify the theoretical prediction as shown in Fig. 3, which indicates the high quality of the generated vector beams. Because the point A represents a linearly polarized vector beam, so $S_3 = 0$. While B is a circular polarized vortex beam, hence

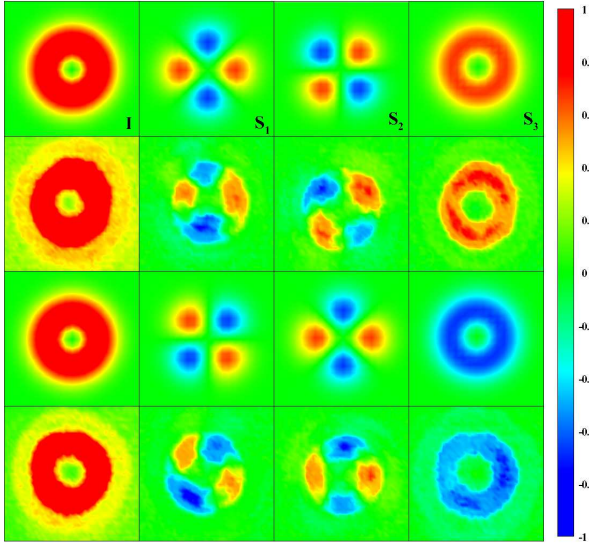


Fig. 4. The Stokes parameters of the generated vector beams corresponding to C and D on the first-order Poincaré sphere (Fig. 1). The first column shows the intensity distribution and the next three columns are the Stokes parameters S_1 , S_2 , and S_3 , respectively. First and third rows: the theoretical results for C and D , respectively. Second and fourth rows: the corresponding experimental results.

$S_1 = S_2 = 0$ and $S_3 = -1$ with its intensity profile equals to the intensity of the beam.

We now expect to obtain vector beams on the points C with $\nu = \pi/4$ and $\phi = 0$, as well as D with $\nu = 3\pi/4$ and $\phi = \pi/2$ as shown in Fig. 1. This two kinds of vector beams can be transformed from the beam on the point A . According to Eqs. (2) and (4), we can generate the beam on the point C by changing the angle α_2 to 49.9° . Similarly, the vector beam on the point D can be realized by rotating the PP1 with $\alpha_1 = 40.1^\circ$ and HH with $\beta = 22.5^\circ$, respectively. All the above transformations to realize the vector beams on points C and D are schematically illustrated in Fig. 1. Then we measure the Stokes parameters of the generated beams (Fig 4). Remarkably, the profile of S_1 and S_2 consists of four intensity lobes and the profile of S_3 exhibits a doughnut shape with a dark center. The experimental results agree well with the theoretical calculations. In order to obtain arbitrary cylindrical vector beams on the first-order Poincaré sphere, we can adjust the optical axis angles of PP1, PP2, and HH.

All the above discussions are limited to the case that the topological charge is $\ell = +1$. Actually, we can also obtain the cylindrical vector beams and realize its evolution on the HOPS by a metasurface [23], but it has less tunable to achieve a cylindrical vector beams with other topological charges ($\ell \neq 1$) than using the SLM. Here, this can be conveniently achieved by modulating the phase picture displayed on the SLM, and all the theoretical and experimental schemes are applicable in this manipulation. To generate the vector beams on the other HOPS with the opposite topological charge $-\ell$, one simple approach is to invert the phase picture on the SLM, and another way is to insert a HWP in each arm of the interfer-

ometer. Note that our scheme can also be applied to generate the vector beams with more complex polarization distribution [24–27].

In conclusion, we have developed a modified Mach-Zender interferometer to generate arbitrary cylindrical vector beams on the HOPS. By suitably modifying the magnitude and phase factors of the interfering beams, we can achieve any desired vector beam on the HOPS. The theoretical prediction is verified by measuring the far-field Stokes parameters. Our scheme makes it possible to generate versatile cylindrical vector beams with high tunability and thereby providing a convenient way to evolve the polarization state in any path on the high order Poincaré sphere.

This research was supported by the National Natural Science Foundation of China (Grants Nos. 11274106, 61025024, and 11347120).

References

1. Q. Zhan, *Adv. Opt. Photon.* **1**, 1 (2009).
2. A. Holleczer, A. Aiello, C. Gabriel, C. Marquardt, and G. Leuchs, *Opt. Express* **1012**, 4578 (2010).
3. G. Milione, H. I. Sztul, D. A. Nolan, and R. R. Alfano, *Phys. Rev. Lett.* **107**, 053601 (2011).
4. F. Cardano, E. Karimi, S. Slussarenko, L. Marrucci, C. de Lisio, and E. Santamato, *Appl. Opt.* **51**, C1 (2012).
5. M. Stadler and M. Schadt, *Opt. Lett.* **21**, 1948 (1996).
6. L. Marrucci, C. Manzo, and D. Paparo, *Phys. Rev. Lett.* **96**, 163905 (2006).
7. W. Han, Y. Yang, W. Cheng, and Q. Zhan, *Opt. Express* **21**, 20692 (2013).
8. R. Oron, S. Blit, N. Davidson, A. A. Friesemt, Z. Bomzon, and E. Hasman, *App. Phys. Lett.* **77**, 3322 (2000).
9. Z. Bomzon, G. Biener, V. Kleiner, and E. Hasman, *Opt. Lett.* **27**, 285 (2002).
10. U. Levy, C. Tsai, L. Pang, and Y. Fainman, *Opt. Lett.* **29**, 1718 (2004).
11. Y. Kozawa and S. Sato, *Opt. Lett.* **30**, 3063 (2005).
12. G. Machavariani, Y. Lumer, I. Moshe, A. Meir, and S. Jackel, *Opt. Lett.* **32**, 1468 (2007).
13. H. Ye, C. Wan, K. Huang, T. Han, J. Teng, Y. S. Ping, and C. Qiu, *Opt. Lett.* **39**, 630 (2014).
14. Q. Zhan, *Opt. Express* **12**, 3377 (2004).
15. Q. Zhan, *Opt. Lett.* **31**, 867 (2006).
16. D. Deng and Q. Guo, *Opt. Lett.* **32**, 2711 (2007).
17. Y. I. Salamin, *Opt. Lett.* **32**, 90 (2007).
18. X. Ling, X. Zhou, H. Luo, and S. Wen, *Phys. Rev. A* **86**, 053824 (2012).
19. L. Yang, X. Xie, S. Wang, and J. Zhou, *Opt. Lett.* **38**, 1331 (2013).
20. L. Allen, M. W. Beijersbergen, R. J. C. Spreeuw, and J. P. Woerdman, *Phys. Rev. A* **45**, 8185 (1992).
21. G. Milione, S. Evans, D. A. Nolan, and R. R. Alfano, *Phys. Rev. Lett.* **108**, 190401 (2012).
22. M. Born and E. Wolf, *Principles of Optics (7th edition)* (Cambridge University Press, Cambridge, 1997).
23. Y. Liu, X. Ling, X. Yi, X. Zhou, H. Luo, and S. Wen, *App. Phys. Lett.* **104**, 191110 (2014).
24. C. Maurer, A. Jesacher, S. Fürhapter, S. Bernet, and M. Ritsch-Marte, *New J. Phys.* **9**, 78 (2007).

25. X. L. Wang, J. Ding, W. J. Ni, C. S. Guo, and H. T. Wang, *Opt. Lett.* **32**, 3549 (2007).
26. L. Chen and W. She, *Opt. Lett.* **34**, 178 (2009).
27. F. Cardano, E. Karimi, L. Marrucci, C. de Lisio, and E. Santamato, *Opt. Express* **21**, 8815 (2013).

References

1. Q. Zhan, "Cylindrical vector beams: from mathematical concepts to applications," *Adv. Opt. Photon.* **1**, 1 (2009).
2. A. Holleczek, A. Aiello, C. Gabriel, C. Marquardt, and G. Leuchs, "Classical and quantum properties of cylindrically polarized states of light," *Opt. Express* **1012**, 4578 (2010).
3. G. Milione, H. I. Sztul, D. A. Nolan, and R. R. Alfano, "Higher-Order Poincaré Sphere, Stokes Parameters, and the Angular Momentum of Light," *Phys. Rev. Lett.* **107**, 053601 (2011).
4. F. Cardano, E. Karimi, S. Slussarenko, L. Marrucci, C. de Lisio, and E. Santamato, "Polarization pattern of vector vortex beams generated by q-plates with different topological charges," *Appl. Opt.* **51**, C1 (2012).
5. M. Stadler and M. Schadt, "Linearly polarized light with axial symmetry generated by liquid-crystal polarization converters," *Opt. Lett.* **21**, 1948 (1996).
6. L. Marrucci, C. Manzo, and D. Paparo, "Optical Spin-to-Orbital Angular Momentum Conversion in Inhomogeneous Anisotropic Media," *Phys. Rev. Lett.* **96**, 163905 (2006).
7. W. Han, Y. Yang, W. Cheng, and Q. Zhan, "Vectorial optical field generator for the creation of arbitrarily complex fields," *Opt. Express* **21**, 20692 (2013).
8. R. Oron, S. Blit, N. Davidson, A. A. Friesemt, Z. Bomzon, and E. Hasman, "Efficient extracavity generation of radially and azimuthally polarized beams," *App. Phys. Lett.* **77**, 3322 (2000).
9. Z. Bomzon, G. Biener, V. Kleiner, and E. Hasman, "Radially and azimuthally polarized beams generated by space-variant dielectric subwavelength gratings," *Opt. Lett.* **27**, 285 (2002).
10. U. Levy, C. Tsai, L. Pang, and Y. Fainman, "Engineering space-variant inhomogeneous media for polarization control," *Opt. Lett.* **29**, 1718 (2004).
11. Y. Kozawa and S. Sato, "Generation of a radially polarized laser beam by use of a conical Brewster prism," *Opt. Lett.* **30**, 3063 (2005).
12. G. Machavariani, Y. Lumer, I. Moshe, A. Meir, and S. Jackel, "Efficient extracavity generation of radially and azimuthally polarized beams," *Opt. Lett.* **32**, 1468 (2007).
13. H. Ye, C. Wan, K. Huang, T. Han, J. Teng, Y. S. Ping, and C. Qiu, "Creation of vectorial bottle-hollow beam using radially or azimuthally polarized light," *Opt. Lett.* **39**, 630 (2014).
14. Q. Zhan, "Trapping metallic Rayleigh particles with radial polarization," *Opt. Express* **12**, 3377 (2004).
15. Q. Zhan, "Properties of circularly polarized vortex beams," *Opt. Lett.* **31**, 867 (2006).
16. D. Deng and Q. Guo, "Analytical vectorial structure of radially polarized light beams," *Opt. Lett.* **32**, 2711 (2007).
17. Y. I. Salamin, "Mono-energetic GeV electrons from ionization in a radially polarized laser beam," *Opt. Lett.* **32**, 90 (2007).
18. X. Ling, X. Zhou, H. Luo, and S. Wen, "Steering far-field spin-dependent splitting of light by inhomogeneous anisotropic media," *Phys. Rev. A* **86**, 053824 (2012).
19. L. Yang, X. Xie, S. Wang, and J. Zhou, "Minimized spot of annular radially polarized focusing beam," *Opt. Lett.* **38**, 1331 (2013).
20. L. Allen, M. W. Beijersbergen, R. J. C. Spreeuw, and J. P. Woerdman, "Orbital angular momentum of light and the transformation of Laguerre-Gaussian laser modes," *Phys. Rev. A* **45**, 8185 (1992).
21. G. Milione, S. Evans, D. A. Nolan, and R. R. Alfano, "Higher

- order Pancharatnam-Berry phase and the angular momentum of Light,” *Phys. Rev. Lett.* **108**, 190401 (2012).
22. M. Born and E. Wolf, *Principles of Optics (7th edition)* (Cambridge University Press, Cambridge, 1997).
 23. Y. Liu, X. Ling, X. Yi, X. Zhou, H. Luo, and S. Wen, “Realization of polarization evolution on higher-order Poincaré sphere with metasurface,” *App. Phys. Lett.* **104**, 191110 (2014).
 24. C. Maurer, A. Jesacher, S. Fürhapter, S. Bernet, and M. Ritsch-Marte, “Tailoring of arbitrary optical vector beams,” *New J. Phys.* **9**, 78 (2007).
 25. X. L. Wang, J. Ding, W. J. Ni, C. S. Guo, and H. T. Wang, “Generation of arbitrary vector beams with a spatial light modulator and a common path interferometric arrangement,” *Opt. Lett.* **32**, 3549 (2007).
 26. L. Chen and W. She, “Electrically tunable and spin-dependent integer or noninteger orbital angular momentum generator,” *Opt. Lett.* **34**, 178 (2009).
 27. F. Cardano, E. Karimi, L. Marrucci, C. de Lisio, and E. Santamato, “Generation and dynamics of optical beams with polarization singularities,” *Opt. Express* **21**, 8815 (2013).